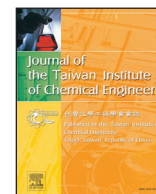




Contents lists available at ScienceDirect

## Journal of the Taiwan Institute of Chemical Engineers

journal homepage: [www.elsevier.com/locate/jtice](http://www.elsevier.com/locate/jtice)

## Blending-induced helical morphologies of confined linear triblock copolymers

Hung-Yu Chang<sup>a</sup>, Yen-Fu Chen<sup>a</sup>, Yu-Jane Sheng<sup>a,\*</sup>, Heng-Kwong Tsao<sup>b,\*</sup><sup>a</sup> Department of Chemical Engineering, National Taiwan University, Taipei 106, Taiwan<sup>b</sup> Department of Chemical and Materials Engineering, Department of Physics, National Central University, Jhongli 320, Taiwan

## ARTICLE INFO

## Article history:

Received 5 March 2015

Revised 27 April 2015

Accepted 3 May 2015

Available online 6 June 2015

## Keywords:

Blending-induced helix

Helical morphology

Confined triblock copolymers

Dissipative particle dynamics

## ABSTRACT

Highly diversified microphase-separated morphologies are readily formed for linear ABC triblock copolymers confined in a cylindrical pore. However, helical morphologies which have potential for the fabrications of metamaterials emerge only at specific block compositions. In this study, we have shown by dissipative particle dynamics simulations the phase behaviors of confined linear triblock copolymers. It is found that helical nanostructures can be induced by blending non-helix-forming triblocks with homopolymers or diblock copolymers. The formation of A/C single helix + B double helices or A/C double helices + B quadruple helices can be precisely controlled by tuning the binary blend ratio to acquire the effective compositions corresponding to those associated with helix-forming pure triblocks.

© 2015 Taiwan Institute of Chemical Engineers. Published by Elsevier B.V. All rights reserved.

## 1. Introduction

Self-assembly under confinement has become a research topic of interest because of the emergence of certain special nanostructures which are unobservable in the bulk phase [1–4]. Features of confined environments, including dimensionality (one-dimensional films, two-dimensional cylindrical channels, and three-dimensional spherical or polyhedral cavities) and surface properties (surface-polymer interactions and deformability), can cause symmetry breaking or structural transformation of the structures formed in unconfined space. Consequently, self-assembled morphologies under spatial confinement are distinct from those in the bulk phase. Numerous experimental and simulation studies on confinement-induced polymeric self-assemblies have been presented [2–7].

Previous studies have primarily focused on diblock copolymers under cylindrical or spherical confining geometries. In cylindrical and spherical confinements with highly selective surfaces, symmetric diblock copolymers typically form concentric sets of cylindrical or spherical shells that are distinct from lamellae parallel in the bulk phase [8–12]. In cases where the confinements are neutral the blocks, however, stacked disks as well as helical and bicontinuous morphologies have been predicted by simulation and theory [10,11]. Novel and hierarchical confined morphologies may exist in triblock copolymer

and polymer blend systems because more interactions and structural parameters are involved compared with those of basic pure diblock copolymer systems [13–16]. Several structures of interest, including core-shell-corona, segmented-worm, hamburger-like and raspberry-like micelles formed by linear ABC triblock copolymers in the selective solvents have been revealed by dissipative particle dynamics (DPD) simulations [17–20]. For the self-assembly of linear or star triblock copolymers in the confined pores, a series of morphological phase diagrams have been established using self-consistent field theory and simulated annealing method [16,21–23]. Moreover, complex self-assembled structures can be generated by diblock copolymer mixtures under various confined conditions [24,25]. For example, morphological transitions from concentric cylindrical barrel structures to screw/cylinder structures and then to stacked disk/cylinder structures upon decreasing the pore diameter have been observed in the binary blends of A<sub>15</sub>B<sub>7</sub> and B<sub>7</sub>C<sub>15</sub> copolymers under cylindrical confinements.

Among all microphase-separated morphologies, helical structures have attracted much attention since they have the potential for the fabrication of electromagnetic wave absorber and metamaterials. Certain helical features such as the number of helical strands, handedness, and pitch are related to the optimal design of electronic devices [26,27]. Until now, it remains challenging to develop the means for the production of helical structures with desired properties. Self-assembly of linear triblock copolymer melts confined in nanocylindrical tubes has been investigated by Monte Carlo simulations [28,29]. Numerous helical morphologies, such as A/B/C double helices, A/C single helix + B double helices, and A/C double helices + B quadruple helices were identified.

\* Corresponding author. Tel.: +886 3 4227151x34226.

\*\* Corresponding author. Tel.: +886 2 33663014; fax: +886 2 23623040.

E-mail addresses: [yjsheng@ntu.edu.tw](mailto:yjsheng@ntu.edu.tw) (Y.-J. Sheng), [hktsao@cc.ncu.edu.tw](mailto:hktsao@cc.ncu.edu.tw) (H.-K. Tsao).

The self-assembled structures of ABC triblock copolymer melts are found to depend on the degree of confinement, chemical nature of each block, and constituent fraction [3,4]. From the viewpoint of structural design, it is important to know whether or not it is possible to have helix morphologies if the triblock copolymer on hand is not helix-forming in a specified degree of confinement. A facile approach to achieve this goal is the polymer blend of triblocks and homopolymers. In this work, dissipative particle dynamic simulations are employed to construct a morphological phase diagram of the triblocks  $A_xB_yC_z$  with various block lengths ( $x$ – $y$ – $z$ ). On the basis of the ternary phase diagram, the possibility of helix formation by blending homopolymers with non-helix forming triblocks is explored.

## 2. Model and simulation method

The dissipative particle dynamics (DPD) is a coarse-grained particle-based approach and allows simulations for longer timescales and wider length scales than atomistic molecular dynamics (MD) [30,31]. Like MD, all DPD beads obey Newton's equation of motion [32,33],

$$\mathbf{f}_i = m_i \frac{d\mathbf{v}_i}{dt}, \quad \mathbf{v}_i = \frac{d\mathbf{r}_i}{dt}. \quad (1)$$

where  $\mathbf{f}_i$  donates the total forces acting on particle  $i$  with mass  $m_i$ .  $\mathbf{v}_i$  and  $\mathbf{r}_i$  are the velocity and position of particle  $i$ , respectively. The force  $\mathbf{f}_i$  exerted on bead  $i$  by bead  $j$  is composed of a conservative force ( $\mathbf{F}_{ij}^C$ ), dissipative force ( $\mathbf{F}_{ij}^D$ ), and random force ( $\mathbf{F}_{ij}^R$ ):

$$\mathbf{f}_i = \sum_{j \neq i} (\mathbf{F}_{ij}^C + \mathbf{F}_{ij}^D + \mathbf{F}_{ij}^R), \quad (2)$$

$$\mathbf{F}_{ij}^C = a_{ij}(\mathbf{r}_c - \mathbf{r}_{ij})\hat{\mathbf{r}}_{ij}, \quad r_{ij} \leq r_c; \quad 0, \quad r_{ij} > r_c, \quad (3)$$

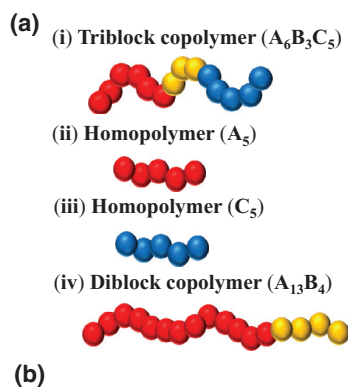
$$\mathbf{F}_{ij}^D = -\gamma\omega^D(r_{ij})(\hat{\mathbf{r}}_{ij} \cdot \mathbf{v}_{ij})\hat{\mathbf{r}}_{ij}, \quad (4)$$

$$\mathbf{F}_{ij}^R = -\sigma\omega^R(r_{ij}) < \text{ct} > \theta < \text{ot} >_{ij}\hat{\mathbf{r}}_{ij}. \quad (5)$$

where  $a_{ij}$  is the maximum repulsion between beads  $i$  and  $j$ ,  $r_{ij} = |\mathbf{r}_i - \mathbf{r}_j|$  is the magnitude of the position vector,  $r_c$  is the cutoff radius,  $\hat{\mathbf{r}}_{ij}$  is the unit vector joining beads  $i$  and  $j$ ,  $\mathbf{v}_{ij} = \mathbf{v}_i - \mathbf{v}_j$ ,  $\theta_{ij}$  is a randomly fluctuating variable with zero mean, and the friction coefficient ( $\gamma$ ) and the noise amplitude ( $\sigma$ ) are parameters coupled by  $\sigma^2 = 2\gamma k_B T$ . The weight functions  $\omega^D$  and  $\omega^R$  are  $r_{ij}$ -dependent, and  $\omega^D = (\omega^R)^2 = (1 - r_{ij}/r_c)^2$  for  $r_{ij} \leq r_c$  and 0 otherwise to satisfy the fluctuation-dissipation theorem. The conservative force  $\mathbf{F}_{ij}^C$  giving chemical identities to non-bonded beads is a soft repulsive force. The dissipative force  $\mathbf{F}_{ij}^D$  acts to reduce the relative momentum between beads  $i$  and  $j$ , while random force  $\mathbf{F}_{ij}^R$  is to impel energy into the system. For applying DPD to our macromolecules, harmonic spring forces ( $\mathbf{F}_{ij}^S$ ) are adopted to bind together the adjacent beads in our system.

$$\mathbf{F}_{ij}^S = -\sum_j C(r_{ij} - r_{eq})\hat{\mathbf{r}}_{ij} \quad (6)$$

where the spring constant is  $C = 100$  and  $r_{eq} = 0.7$  denotes the equilibrium length. The spring force is used to impose connectedness among beads in a polymer, and the choice of  $C$  and  $r_{eq}$  will not influence the qualitative behavior of the system studied in our work. For all the DPD simulations presented here, all units are scaled by  $m$ ,  $k_B T$  and  $r_c$  and they are conveniently taken as  $m = k_B T = r_c = 1$ . As a result, the force acting on a bead equals its acceleration. All the forces except for the harmonic spring forces come to zero outside a certain  $r_c$ . Newton's equation of motion is integrated using the modified velocity Verlet algorithm [32] with  $\lambda = 0.65$  and time step  $\Delta t = 0.04$ . Since



$a_{ij}$	W	A	B	C
W	25	30	40	26
A		25	50	40
B			25	50
C				25

Fig. 1. (a) Schematic diagrams of four types of model polymers (b) the interaction parameters ( $a_{ij}$ ) between cylindrical channel (W) and different components of polymers.

DPD simulation utilizes soft-repulsive potentials, the systems studied are allowed to evolve much faster than the “brute-force” molecular dynamics. A typical DPD simulation requires only about  $10^5$  steps to equilibrate. Therefore, each simulation in this work takes at least  $5 \times 10^5$  steps and the first  $1 \times 10^5$  steps are for equilibration.

In this work, microphase-separated morphologies of linear  $A_xB_yC_z$  triblock copolymers confined in a cylindrical channel is investigated. As shown in Fig. 1a,  $A_x$ ,  $B_y$ , and  $C_z$  denote A block with  $x$  beads, B block with  $y$  beads, and C block with  $z$  beads, respectively. The channel wall is also constructed by DPD beads and the diameter of the nanopore scaled by the bead diameter is 23 (see Fig. S1 of the supplementary materials). The repulsive interaction parameters ( $a_{ij}$ ) are shown in Fig. 1b. These  $a_{ij}$  are chosen in an attempt to retain the characteristic interactions associated with each component of the system studied. Typically,  $a_{ij}$  for beads of the same type is taken as  $a_{ii} = 25$  and the cross terms are chosen as  $a_{ij} = 25 + \Delta a$ , where  $\Delta a$  defines the excess repulsion and can be obtained from Flory–Huggins parameter  $\chi$ . As the incompatibility between beads  $i$  and  $j$  grows,  $\Delta a$  increases. Note that  $a_{wi}$  depicts the interaction between the channel wall (W) and bead  $i$ . A, B, and C-blocks are incompatible to one another and B-blocks are strongly repelled from the wall. An example of our simulation system is poly(methyl methacrylate)-*b*-poly(styrene)-*b*-poly( $\epsilon$ -caprolactone) in nanopores of anodic aluminum oxide. Note that for each case, we have performed several simulations from different initial configurations. It is found that the final states are the same irrespective of the initial conditions. The outcome indicates that a true equilibrium state is reached.

## 3. Results and discussion

### 3.1. Ternary phase diagram of linear ABC triblock copolymers

In order to systematically study the effects of the block compositions (lengths) on the self-assembled morphologies of linear ABC triblock copolymers under cylindrical confinement, a ternary phase diagram is constructed, as shown in Fig. 2. The compositions of A, B, and C blocks related to the block lengths by  $f_A = x/(x + y + z)$ ,  $f_B = y/(x + y + z)$ , and  $f_C = z/(x + y + z)$ . Our simulations reveal that helical structures emerge as the B block is short. Therefore,  $f_A$  and  $f_C$  are varied from 0.10 to 0.75, while that of  $f_B$  is set only in the range of 0.10–0.30. Nine distinct equilibrium morphologies are observed and the characteristic snapshots of the overall view and individual

Download English Version:

<https://daneshyari.com/en/article/690632>

Download Persian Version:

<https://daneshyari.com/article/690632>

[Daneshyari.com](https://daneshyari.com)